ADC Compensation Using A Sinewave Histogram Method

By
Jonathan Larrabee

B.S. University of Maine, 1995

A THESIS
Submitted in Partial Fulfillment of the
Requirements for the Degree of
Master of Science
(in Electrical Engineering)

The Graduate School
University of Maine
August 1997

Advisory Committee:

Donald M. Hummels, Associate Professor of Electrical and Computer Engineering, Thesis Advisor

Fred H. Irons, Castle Professor of Electrical and Computer Engineering,

Allison I. Whitney, Lecturer in Electrical and Computer Engineering.

LIBRARY RIGHTS STATEMENT

ADC Compensation Using A Sinewave Histogram Method

By Jonathan Larrabee

Thesis Advisor: Donald M. Hummels, Ph.D.

An Abstract of the Thesis Presented

in Partial Fulfillment of the Requirements for the

Degree of Master of Science

(in Electrical Engineering)

August 1997

This thesis describes a new method for developing ADC error function models using standard sinewave histogram methods. The histograms supply information to accurately estimate expected error for each ADC output code. The method provides better error representation by providing error basis functions for every output code. Results show this method is capable of removing all slope dependent errors in complex ADC error models and application to a 200 MSPS ADC showed more than 10 dB improvement in SFDR over the full Nyquist band for the ADC.

ACKNOWLEDGMENTS

This work has been supported in part by the ARPA HBT/ADC program under a contract administered by the Office of Naval Research Grant N000149311007 and the DEPSCoR program through the Army Research Office Grant DAAH04-94-G-0387

I would like to thank the University of Maine for giving me a pleasant educational experience and my parents for paying for it.

TABLE OF CONTENTS

LIST OF FIGURES

CHAPTER 1

Introduction

The need for high dynamic range analog-to-digital converters (ADCs) is strong due to the growing use of digital signal processing in communications applications. The analog signals must be converted into digital form before any digital processing can begin. The conversion is not ideal and error is introduced by the ADCs used in the process. This thesis develops an error model, to accurately describe error introduced by an ADC, as a function of output code and input signal slope. This error model is then applied to the ADC in order to remove harmonic distortion introduced by the converter.

1.1 Background

Modeling ADC error as a function of state (ADC output code) and slope of the input signal is not a new concept [4, 9, 7]. Previous compensation schemes use smooth basis functions over output code and input signal slope to describe ADC error. An error table is created and the sample and input signal slope index an error value from the table to be subtracted from the sample. There have been different approaches to forming an estimate of ADC error. Neural networks have been used to track ADC error using a technique called the fast orthogonal search [2]. The fast Fourier transform (FFT) has been used to observe and estimate harmonic distortion introduced by the converter [7]. For these procedures, the ADC is driven with a single tone sinusoid and the FFT spectrum is created from the converter output. The components of the spectrum that are above the noise floor (other then the two fundamental terms and the dc term) are considered ADC error and the look-up table is generated from these error terms [4].

1.2 Purpose of the Research

This thesis describes a new calibration method for finding ADC error functions. The method is based upon expected error for each state of the converter. The error for each state is estimated as a function of the slope of the input to the ADC. Sinewave histogram techniques are then used to obtain estimates of expected error which are used to form curve fits of error-versus-slope for each state. The functions used to estimate error in previous compensation methods are found from averaging over a range of states and slopes [4, 9, 7]. It will be shown later in this thesis that ADC error contains discontinuous jumps from state-to-state and these discontinuities can not be accurately described when error is averaged over a range of states. This thesis develops a procedure which in this thesis allows a smooth error function in slope for each state. By increasing resolution in the state domain, discontinuous jumps in error, from state-to-state, are accurately modeled thus improving the ADC error representation capabilities of the model.

1.3 Thesis Organization

This thesis sets up necessary procedures needed to implement an error compensation method on real ADCs.

Chapter 2 describes and develops the ADC error model used in this thesis. The model describes dynamic error for each output state as a function of the slope of the input signal. Chapter 2 also describes a method of using histograms of the output sample sets to measure error introduced by the converter. The histogram is used to estimate the quantization thresholds of the converter which is crucial in estimating basis function coefficients.

Chapter 3 shows how to calibrate ADCs to obtain valid information for building dynamic error models. This chapter also presents a procedure to estimate the error function basis coefficients using the calibration data. It is found that for each calibration signal, there exists two unknown parameters, namely : the amplitude and dc offset of the input signal. Constrained least-squares approach is used to estimate these parameters so the error function basis coefficients can be estimated.

Chapter 4 describes how to compensate a raw ADC sample set using the error model developed in Chapter 3. The effectiveness of the error model, developed in this thesis, is evaluated through the use of simulated ADC performance to show that the proposed method removes all output code and slope dependent errors from output sample sets. The error compensation method is then applied to a real wide-band 8-bit flash ADC where it is found that performance is improved over the full Nyquist band of the ADC.

Chapter 5 contains conclusions for this thesis.

CHAPTER 2

ADC Error Modeling

In theory, analog-to-digital conversion transforms continuous time signals into signals that exist on equally spaced time intervals at discrete output values. When the conversion is ideal, the only error introduced by this process is quantization error from the digitization of the analog signal. By using a dithered input signal to randomize error, quantization error is made to appear as additive noise, with a noise level that depends on the resolution of the ADC [3]. However, most conversion is not ideal and errors resulting from ADC architectural non-linearities are introduced. This chapter develops a generic error model for non-ideal ADC performance.

2.1 Error Model as a Function of Output Code

The first error model developed in this chapter is a function of ADC output code. Errors contributed by the voltage reference of the ADC fall in this category. By exciting an ADC at or near its full input range and measuring the corresponding output codes, an ADC transfer function can be determined. From this transfer function, output code versus input voltage, ADC static error patterns may be defined.

2.1.1 ADC Transfer Function

ADC performance can be described in terms of the transfer function of output code versus input voltage [1]. Fig. 2.1 shows a non-ideal transfer function relating input voltage to ADC output codes. Each ADC output code, i, is associated with two input voltage thresholds, t_i and t_{i+1}. These quantization thresholds describe the range of input voltage that yields the ith output code. By observing

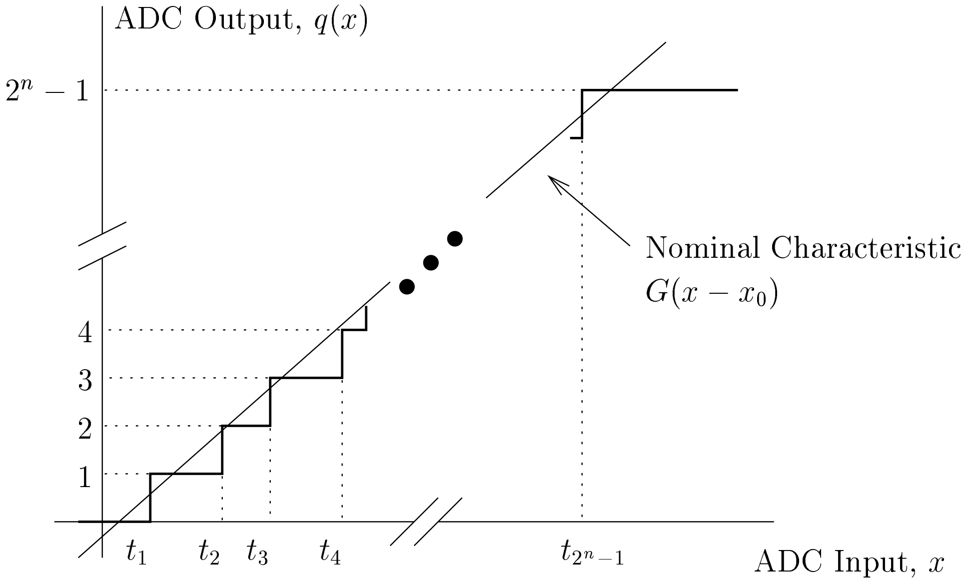

Figure 2.1: Non-Ideal ADC transfer function

all output codes versus their input voltage thresholds, the ADC transfer function is created. For an ideal converter, the quantization thresholds are equally spaced, so that the ADC output code is roughly proportional to the ADC input voltage. Non-ideal devices have a non-linear relationship between input voltage and output code, which is an attempt to approximate a desired linear curve. For a given ADC transfer characteristic, the "Nominal Characteristic" is defined as the straight line relationship which the ADC approximates. In Figure 2.1 this characteristic is shown as a line with slope G and intercept x_o. One common measure of ADC quality is the expected error characteristic. Expected Error is a function of the ADC output state, and is defined by the average deviation of the ADC transfer function from the nominal characteristic for state i. Fig. 2.2 shows the ADC error ($e(x)$) as a function of input voltage (x), and it is constructed by subtracting the nominal characteristic, $G(x - x_o)$, from the transfer function and zooming in on the ith output state. The average error for state i is referred to as expected error, and is denoted by E_i. The expected error for state i may be written in terms of

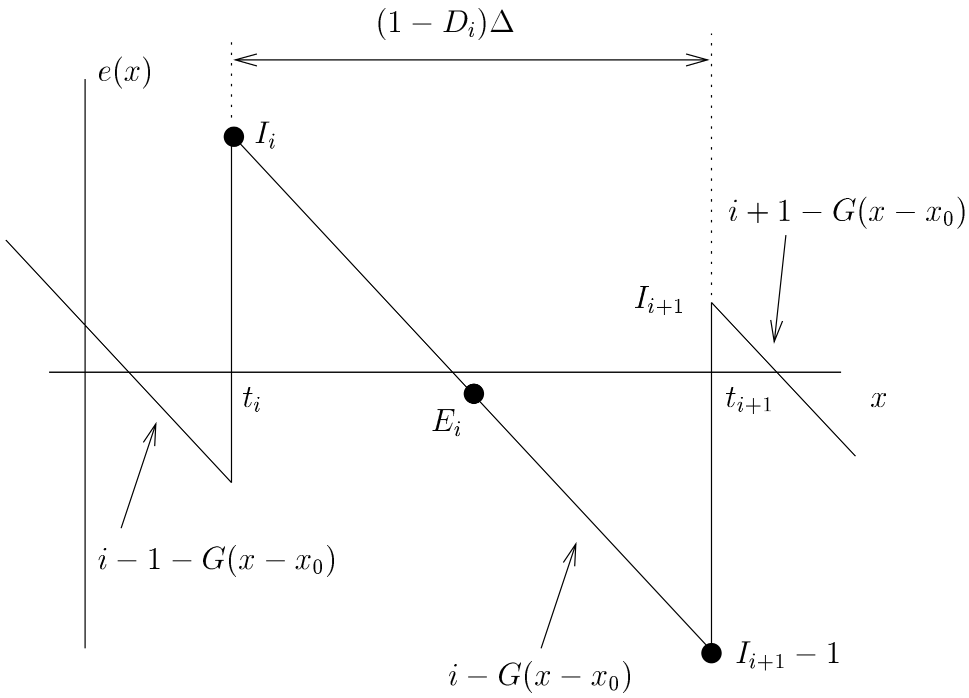

Figure 2.2: Static error description

the quantization thresholds t_i by finding the midpoint of the error curve shown in Fig 2.2.

$$E_i = i - G\left(\frac{t_i + t_{i+1}}{2} - x_o\right). \quad i = 1, 2, \ldots, 2^n - 2 \tag{2.1}$$

G and x_o are the gain and offset of the nominal characteristic, n is the number of bits for the ADC, and t_i, t_{i+1} are quantization thresholds that yield the ith output state. Equation (2.1) gives the expected error as a function of output code in terms of the quantization thresholds t_i and t_{i+1}. A method for estimating quantization thresholds must be determined in order to use (2.1).

2.1.2 Histogram Methods

Histogram tests offer a way to estimate quantization thresholds which is necessary in order to estimate the expected error of (2.1). Creating a histogram over an ADC output sample set involves counting how many times each output code occurs. A relationship between the number of occurrences for state i relative to the total number of samples in the set and the width of state i $(t_{i+1} - t_i)$ may be established. The quantization intervals are bordered by quantization thresholds t_is. For example, if a ramp input is applied to an ADC, and a large number of samples are collected, then ideally each state i should contain the same number of occurences. If one state contains fewer occurences than the average, its quantization width $(t_{i+1} - t_i)$ is smaller than the average width. Similiarly, if a state's number of occurences is large, then its quantization interval is large. If enough samples are obtained, accurate estimates of quantization thresholds are determined. For a generic input signal, quantization thresholds can be estimated by relating the histogram of collected samples to the expected histogram of an ideal converter which is defined by the characteristics of the generic input signal.

Knowing the type of input signals to the ADC, a formal procedure for estimating thresholds is developed. Assume the values (voltages) of the input sinusoid to an ADC are denoted by the random variable X, then its distribution function is as shown in Fig. 2.3. Where A is the sinewave amplitude and c is its DC offset. Now let Y represent the random variable of the non-ideal quantizer output. Y takes on integer values of $0, 1, 2, \ldots, 2^n - 1$ and its distribution function may be estimated from the histogram performed on the sample set. Given a set of N samples, the estimated distribution function is given by $\hat{F}_Y(i) = \frac{S_i}{N}$, Where S_i is the cumulative number of occurences for output codes 0 to i. The distribution function for Y is discrete as shown in Fig.2.4.

The distribution functions of X and Y are related by the values of the quantization thresholds, t_i :

$$\begin{aligned} F_X(t_i) &= P(X \leq t_i) \\ &= P(Y \leq i - 1) \end{aligned}$$

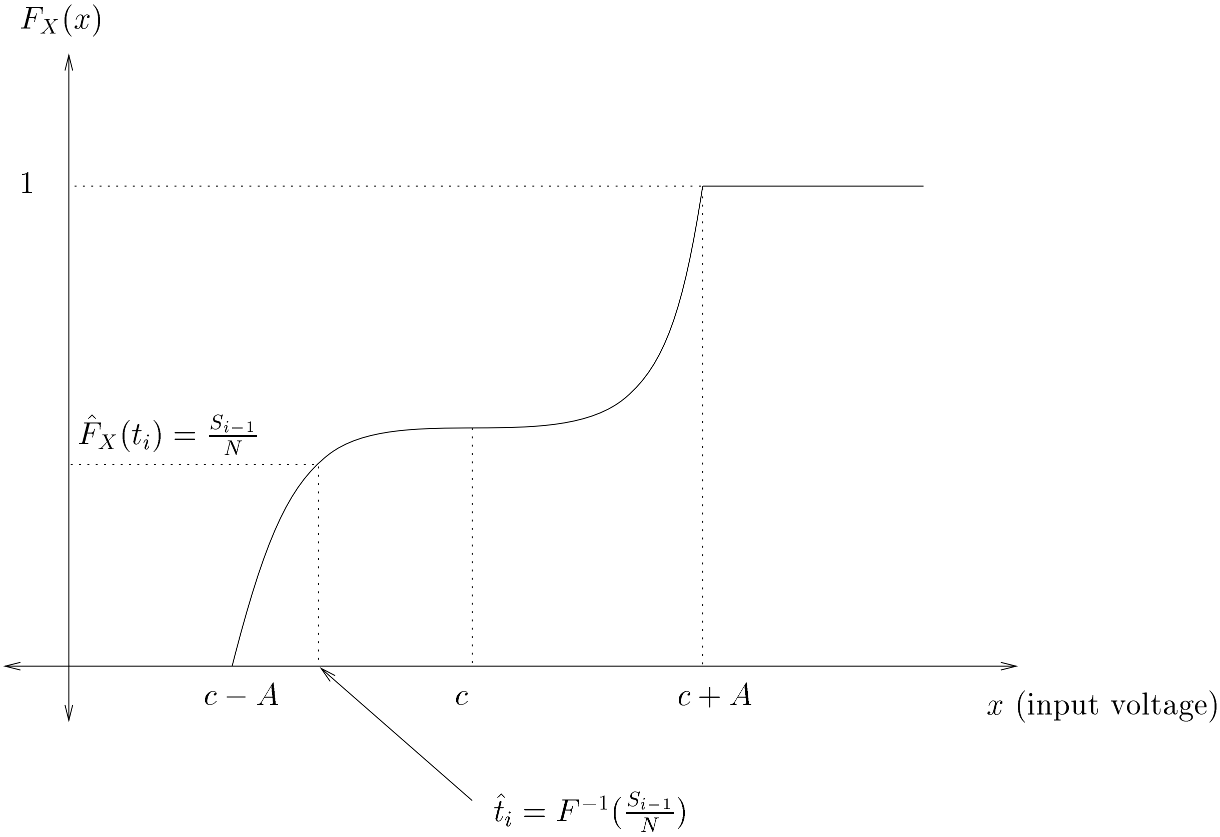

Figure 2.3: Distribution function for sinewave input

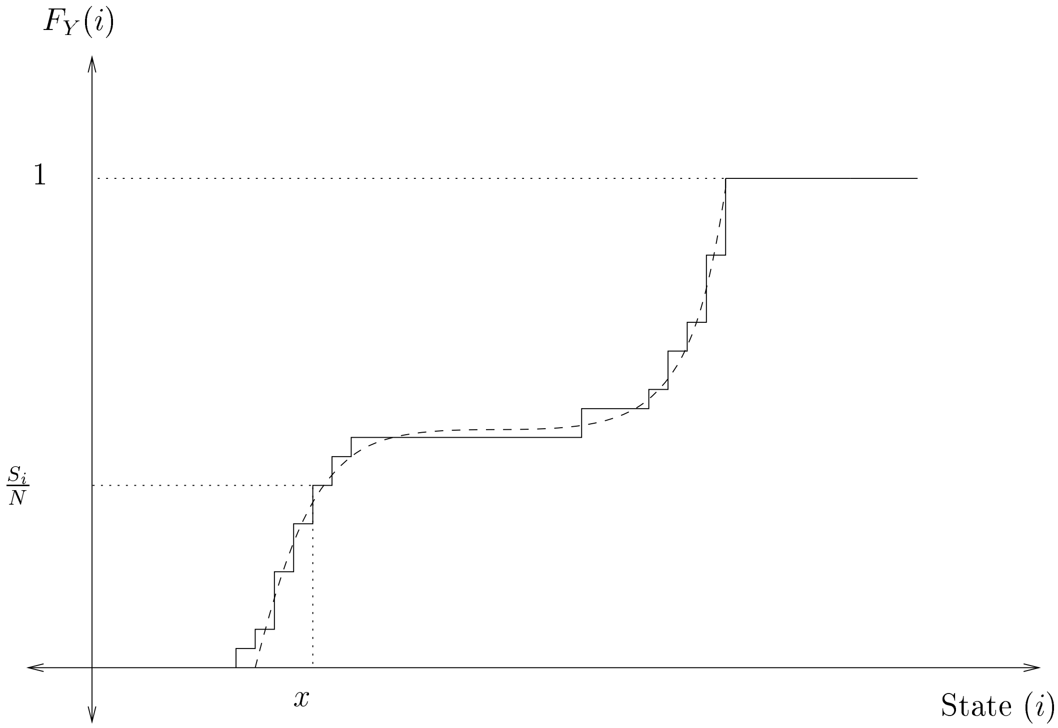

Figure 2.4: Distribution function for quantized output of sinewave input

$$= \quad F_Y(i-1).$$

An estimate of the threshold, t_i, may be obtained by using the estimated distribution of Y and the known functional form for $F_X(x)$

$$F_x(\hat{t}_i) = \frac{S_{i-1}}{N}. \tag{2.2}$$

Solving this relationship for $\hat{t}_i$ and an expression for the estimated quantization thresholds is determined from a histogram of the output sample set [1].

2.1.2.1 Implementation Using Sinewaves

The test signals used to implement procedures in this thesis are sinusoidal. The distribution function for a sinusoidal signal is given by 2.3.

$$F_x(\hat{t}_i) = \frac{1}{2} + \frac{1}{\pi}\arcsin\left(\frac{\hat{t}_i - c}{A}\right) \tag{2.3}$$

Where A and c are the amplitude and offset of the input sinusoid. Substituting 2.3 into (2.2) and solving for t_i gives 2.4.

$$\hat{t}_i = -A\cos\left(\pi\frac{S_{i-1}}{N}\right) + c. \quad i = 1, 2, \ldots, 2^n - 1 \tag{2.4}$$

N is the number of samples in the set. A description for the estimated expected error of a particular ADC output code is obtained by combining (2.1) with (2.4) which yields (2.5).

$$\hat{E}_i = i + GA\left(\frac{\cos\left(\pi\frac{s_{i-1}}{N}\right) + \cos\left(\pi\frac{s_i}{N}\right)}{2}\right) - G(c - x_o). \tag{2.5}$$

Equation (2.5) contains two unknown parameters, (GA) and $(G(c - x_o))$. The input-voltage-to-ADC-output-code transfer function parameters, G and x_o, for a single input sinusoid are not known exactly. The exact amplitude, A, and DC offset, c, of the input sinusoid is also difficult to control and know with sufficient accuracy. Both the converter circuitry and the test setup can introduce gain and offset errors to the input signal of the ADC. A method for estimating the unknowns of (2.5) will be developed in Chapter 3.

For a single test sinusoid, the unknowns A and c can be estimated from an FFT of the sample set. Two common methods can be used to estimate the nominal characteristics of the ADC transfer function [1]. The independent-based method chooses G and x_o to minimize the sum-squared expected error over all states. The terminal-based approach selects G and x_o that zeros the error (nominal characteristic subtracted from the non-ideal ADC transfer function) at t_1 and t_{2^n-1} to obtain 2.6.

$$\begin{aligned} G &= \frac{2^n - 2}{t_{2^n-1} - t_1} \\ x_o &= t_1 - \frac{1}{G} \end{aligned} \tag{2.6}$$

The G and x_o are global parameters so that when dealing with several sets of calibration data, neither method is practical when used independently on each sinusoid because each set yields different values for G and x_o. This problem will be examined in more detail later in Chapter 3.

2.1.3 Incomplete Error Model

An important characteristic of expected error for an ADC must be discussed. For practical converters, the expected error for an ADC depends on the dynamic behavior of the input signal. Fig. 2.5 shows estimated expected errors for the full range of a Tektronics AD-20 8-bit ADC for a single sinusoidal input. The samples were divided into two sets based upon the polarity of the slope of the sampled signal. The sorting is achieved by obtaining a slope estimate associated with each sample and separating the samples into positive and negative slope sets. The terminal-based approach [1] is used to estimate parameters, G and x_o, and (2.5) is used to obtain expected errors for each sample set. The terminal-based method chooses the nominal characteristic based on the first and last quantization thresholds. G and x_o are selected so that the nominal curve of Fig.2.1 passes through the top of the risers at each of these transition locations. In other words, the linear nominal characteristic curve contains the two points $(t_1, 1)$ and $(t_{2^n-1}, 2^n - 1)$. From Fig.2.5 it is evident that estimated expected error follows a different pattern

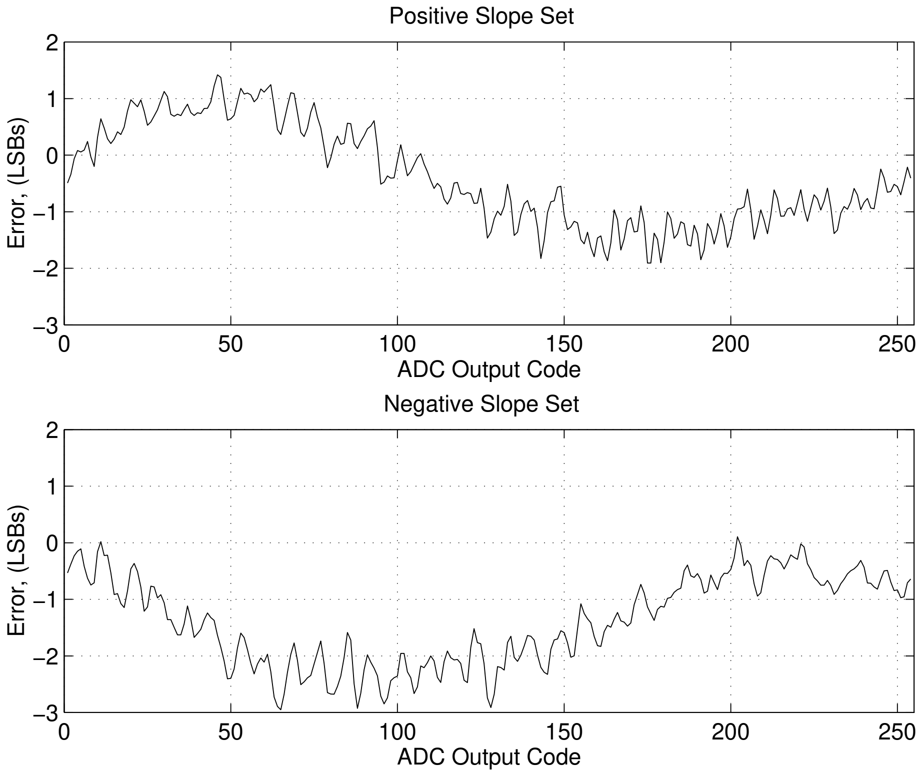

Figure 2.5: Estimated expected error for positive and negative slope sample sets

for the positive slope set than that of the negative slope set, and the pattern also changes with frequency. The error model described by 2.5 is incomplete. It has no apparent input signal slope dependency associated with it. The following section deals with this deficiency.

2.2 Error Model as a Function of ADC Output and Signal Slope

Dynamic performance is described as the behavior of the ADC when time varying signals are present at the input rather than static or constant slope signals. As pointed out in the previous section, estimated expected error not only depends on the input voltage level of the signal but it also depends on whether the input signal is decreasing or increasing at a given magnitude. Parameters used in this thesis to describe dynamic error characteristics are the slopes of the input signal and the corresponding output code states. In this thesis, a separate error function $e_i(y)$ is used for each converter output code, where i denotes the output code, and y represents the corresponding input signal slope. This model is a departure from previous ADC error models [6] [5] which employed smooth functions of both output code and input slope. By using separate error functions for each output code, highly discontinuous error functions reflecting differential ADC errors may be developed. These discontinuous error functions are common for many ADC architectures.

To solve for the desired error function, each function $e_i(y)$ is written in 2.7 as a linear combination of a set of basis functions.

$$\hat{e}_i(y) = \sum_{k=1}^{M} \alpha_{i,k} b_k(y) \tag{2.7}$$

$\hat{e}_i(y)$ is estimated expected error at state i evaluated at slope y, $b_k(y)$ is the k_{th}

basis function evaluated at slope y, and $\alpha_{i,k}$ is the k_{th} basis function coefficient for state i. There are 2^n sets of basis function coefficients possible since a set is defined for each output state of the ADC. Equation (2.7) yields an error function of slope for every state of the converter. It has been shown that practical converters exhibit discontinuous error-versus-slope patterns between adjacent output codes. Allowing separate error-versus-slope functions for every state should increase the effectiveness of these error models relative relative to previous methods. A variety of basis functions can be used in 2.7 to describe the dynamic error.

A model for estimated expected error as a function of output code and signal slope has been presented. The next chapter develops procedures to estimate the combined parameters, G and x_o, of 2.5 and the basis function coefficients of (2.7) for each state and data set.

CHAPTER 3

Calibrating The ADC

In Chapter 2 an error model dependent on output code and signal slope was developed. This chapter describes how to use measured ADC data to estimate the model parameters. Data must be collected from the ADC to accurately characterize the converter according to the proposed error model. Sinusoids are the chosen input signals to implement ADC error development in this thesis. They exhibit dynamic behavior for use in the error model and may be generated with good fidelity in a laboratory. The amplitudes and frequencies of the sinusoids must be carefully selected for accurate ADC characterization. Section 3.1 will show how to drive the ADC with a range of sinusoids that span its full range of output codes and signal slopes. Once data are collected, they must be manipulated into a useful form for developing error basis function coefficients. The remainder of this chapter addresses the steps of collecting raw ADC sample sets and using the collected data to estimate ADC error as a function of state and slope.

3.1 Output Code and Slope Space

Calibration of an ADC involves the selection of the model parameters, $\alpha_{i,k}$ in (2.7), to predict expected errors for the ADC. Sinewave histogram techniques are used to accomplish this task. To accurately describe error, the ADC must be excited over its full range of state and slope values. Error observed in response to applied test signals determines appropriate coefficients for the basis functions used in (2.7).

Each sinusoidal test signal generates an elliptical trajectory in state and slope space. Varying the amplitude and frequency of a sinusoid changes the shape of the ellipse. Large frequencies create greater ranges in slope values and large

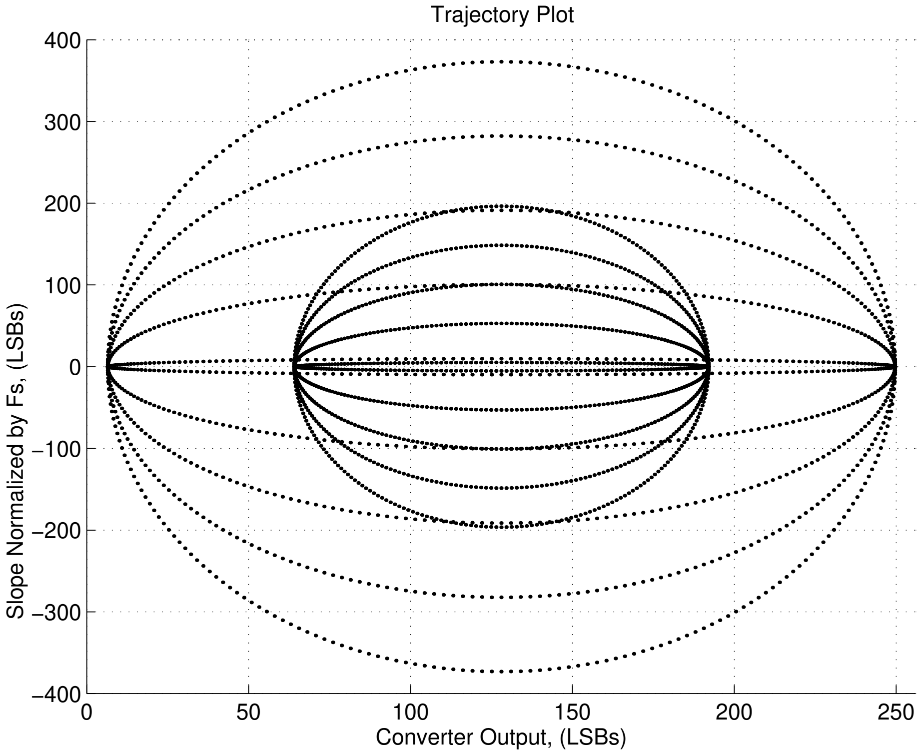

Figure 3.1: Trajectory plot using 5 frequencies at 2 amplitudes per frequency

amplitudes excite more output codes. Choosing various frequencies and amplitudes yields a series of trajectories as shown in Fig. 3.1. The goal is to choose a series of sinusoids at varying amplitudes and frequencies that fill the state and slope space (the domain of the error model) while providing intersections that help reduce error ambiguities in the least-squares estimation of the basis function coefficients. These sets are used to obtain an estimate of the basis function coefficients of (2.7).

3.2 Calibration Overview

A large number of samples are collected for each sinusoidal input to the ADC. Slope estimates are obtained from the samples and separate histograms are constructed based upon positive and negative slopes to form estimates of the expected error for the upper and lower half of each trajectory. For example, in this thesis, the number of samples collected for each trajectory is 16k. This leaves roughly 8k samples in each of the positive and negative slope sets. There are 256 output codes on an 8-bit ADC and so the 8k samples are spread out over 256 bins when a histogram is constructed. There must be enough occurences (S_i) for each output code in order to obtain an accurate estimate of the quantization thresholds, ($\hat{t}_i$). For an 8-bit converter, 16k samples are just enough to ensure that each bin of the histogram has enough occurences for both positive and negative slope sets. Each trajectory introduces two parameters, (GA) and ($G(c - x_o)$), as shown in (2.5). The data collected from each trajectory contains information that is used to solve for the basis function coefficients, $\alpha_{i,k}$.

3.3 Estimating Thresholds

A single trajectory yields two histograms, one for positive sloped samples and one for negative sloped samples. Equation (2.4) gives an expression for estimating thresholds based on the sums, S_{i-1}, obtained from the histogram. However, the amplitude and offset, A and c of the input sinusoid are usually unknown. The converter setup and test procedure can introduce amplitude distortion and DC offset. The quantity $\cos\left(\pi\frac{S_{i-1}}{N}\right)$ in (2.4) is known and can be found from both histograms of a single trajectory. Each histogram constructed from a trajectory yields the quantity

$$\frac{\cos\left(\pi\frac{S_{i-1}}{N}\right) + \cos\left(\pi\frac{S_i}{N}\right)}{2}$$

in (2.5). The unknowns, (GA) and ($G(c-x_o)$), and $\alpha_{i,k}$ still need to be determined to complete this story.

In implementation, significant memory savings may be realized by reducing the data prior to estimation of the error terms. The goal is to construct a single error term based on state i and slope y, from (2.7). For example, a single trajectory of 16k samples results in two sample sets (positive and negative sloped) of roughly 8k samples per set. The corresponding slope estimates are of length 8k for each of these sets. However, when the two histograms are constructed the 16k sample set is condensed down to two histograms vectors each of length 2^n where n is the number of converter bits. For every output code i, two slope estimates ,y, are obtained, one for positive and one for negative slope sample sets. For both positive and negative slope sets, the slopes that correspond to state i are averaged to yield one average slope estimate for state i. For sinusoidal calibration signals, the slopes that correspond to a particular output code should be nominally equal for a fixed trajectory.

3.4 Estimation of Basis Coefficients

The following test outlines a procedure developed to achieve estimates for all $\alpha_{i,k}$. A complete description of the required mathematics will be presented later in section 3.4.2. The goal of this calibration scheme is to estimate expected error as a function of slope for each state of the ADC. In order to calculate estimated expected error it is necessary to solve for (GA) and $(G(c - x_o))$ in (2.5) for each trajectory. This is accomplished by first finding (GA) and $(G(c - x_o))$ for one arbitrarily selected reference trajectory using the independent-based method [1]. By setting (2.5) equal to (2.7) for all states and finding a least-squares solution for the basis coefficients (α's), an expression is obtained for the basis coefficients for all states as a function of the (GA) and $(G(c-x_o))$ terms in (2.5) for all trajectories. A least-squares solution is then obtained to minimize the model error over all values of (GA) and $(G(c-x_o))$. The minimization is performed under the constraint that the unknowns found for the reference trajectory remain fixed. The result is an expression which yields (GA) and $(G(c - x_o))$ for all the trajectories. Using these estimates, the $\alpha_{i,k}$ terms of (2.5) may then be obtained. These values, in turn are used to calculate the error characteristic as a function of state and slope.

3.4.1 Conventional Method and Its Problems

A conventional way of estimating the unknowns in (2.5) is to use the FFT of the samples to obtain estimates for c and A and to use a terminal or independent-based method [1] to estimate G and x_o. This procedure could be used individually for each trajectory and the resulting estimated parameters could be used to calculate estimated expected error from (2.5). Every ADC output state i excited by a trajectory has two slope and error terms associated with it. For state i the basis functions of (2.7) could then be used to "best" fit a curve versus slope to the expected error of (2.5). The result of this procedure would give a description of expected error based on state and slope of the input. However, experiments have shown that this method for finding c, A, G, and x_o individually for each trajectory causes a severe degradation in the error model accuracy. The degradation is due to the fact that G and x_0 are global parameters of the ADC and need to be estimated over the entire dynamic range of state and slope, rather than just for a single trajectory. A different approach must be used to estimate the unknown parameters, (GA) and $(G(c - x_o))$.

3.4.2 Solving For (GA) and $(G(c - x_o))$

The following sections give a mathematical description on how to estimate the basis function coefficients.

Equation (2.5) may be rewritten

$$\hat{E}_i = i - p_1 h_i - p_0, \tag{3.1}$$

where

$$p_0 = G(c - x_o), \quad p_1 = GA$$

$$h_i = -\frac{\cos\left(\pi\frac{s_{i-1}}{N}\right) + \cos\left(\pi\frac{s_i}{N}\right)}{2}. \tag{3.2}$$

$\hat{E}_i$ is the estimated expected error for output code i, p_0 and p_1 are unknowns, and h_i is found from a histogram. A method for estimating these unknowns is developed as follows.

3.4.2.1 Solving For α's in Terms of p_1 and p_0

From Chapter 2 an error model as a function of output code and signal slope was developed and is described by $\hat{e}_i(y) = \sum_{k=1}^{M} \alpha_{i,k} b_k(y)$. A vector form of this model is described by the following

$$\begin{aligned} \hat{e}_i(y) &= \begin{bmatrix} b_1(y) & b_2(y) & \ldots & b_M(y) \end{bmatrix} \cdot \begin{bmatrix} \alpha_{i,1} \\ \alpha_{i,2} \\ \vdots \\ \alpha_{i,M} \end{bmatrix} \\ &= \vec{b}^T(y) \cdot \vec{\alpha}_i \end{aligned} \tag{3.3}$$

Each trajectory has two estimated expected error terms, per output code i, associated with it, one term for positive and one for negative sloped samples. Setting both of the estimated errors of (2.5) equal to the estimated errors of (2.7) yields 3.4.

$$\begin{aligned} i - h_i^{+jth} p_1^{jth} - p_0^{jth} &\approx \vec{b}^T(y_i^{+jth}) \cdot \vec{\alpha}_i \\ i - h_i^{-jth} p_1^{jth} - p_0^{jth} &\approx \vec{b}^T(y_i^{-jth}) \cdot \vec{\alpha}_i \end{aligned}$$

$$i\begin{bmatrix}1\\1\end{bmatrix}-\begin{bmatrix}1 & h_i^{+jth}\\1 & h_i^{-jth}\end{bmatrix}\cdot\begin{bmatrix}p_0^{jth}\\p_1^{jth}\end{bmatrix}\approx\begin{bmatrix}\vec{b}^T(y_i^{+jth})\\\vec{b}^T(y_i^{-jth})\end{bmatrix}\cdot\vec{\alpha}_i \tag{3.4}$$

The $+jth$ and $-jth$ superscripts indicate the positive and negative sloped portions of the jth trajectory. p_0^{jth} and p_1^{jth} are the global unknown parameters associated with the jth trajectory. These terms are the same for both positive and negative sloped sample sets since the sets came from the same input sinusoid. The problem at hand is to solve for the basis function coefficients, $\vec{\alpha}_i$, $(i = 1, 2, \ldots, 2^n - 2)$, and the unknown trajectory parameters p_0^{jth} and p_1^{jth} which minimizes the error in the approximation of (3.4). y_i^{+jth} and y_i^{-jth} are the average positive and negative slopes for output code i of the jth trajectory. h_i^{+jth} and h_i^{-jth} terms are constructed from the positive and negative slope histograms respectively. The relationship described by (3.4) is expanded over all the trajectories that drive the ADC creating the relationship given in 3.5.

$$i\cdot\begin{bmatrix}1\\1\\1\\1\\\vdots\\1\\1\end{bmatrix}-\begin{bmatrix}1 & h_i^{+1st} & 0 & 0 & \ldots & 0 & 0\\1 & h_i^{-1st} & 0 & 0 & \ldots & 0 & 0\\0 & 0 & 1 & h_i^{+2nd} & \ldots & 0 & 0\\0 & 0 & 1 & h_i^{-2nd} & \ldots & 0 & 0\\\vdots & \vdots & \vdots & \vdots & \vdots & \vdots & \vdots\\0 & 0 & 0 & 0 & \ldots & 1 & h_i^{+kth}\\0 & 0 & 0 & 0 & \ldots & 1 & h_i^{-kth}\end{bmatrix}\cdot\begin{bmatrix}p_0^{1st}\\p_1^{1st}\\p_0^{2nd}\\p_1^{2nd}\\\vdots\\p_0^{kth}\\p_1^{kth}\end{bmatrix}\approx\begin{bmatrix}\vec{b}^T(y_i^{+1st})\\\vec{b}^T(y_i^{-1st})\\\vec{b}^T(y_i^{+2nd})\\\vec{b}^T(y_i^{-2nd})\\\vdots\\\vec{b}^T(y_i^{+kth})\\\vec{b}^T(y_i^{-kth})\end{bmatrix}\cdot\vec{\alpha}_i$$

$$i\cdot\vec{1}-\mathbf{H}_i\cdot\vec{p}=\mathbf{B}_i\cdot\vec{\alpha}_i \tag{3.5}$$

The bottom expression is the matrix form for the top expression. Examining the matrix $\mathbf{H}_i$ shows that each trajectory composes a 2×2 sub-matrix within $\mathbf{H}_i$. Not all output codes are excited by a particular trajectory due to the amplitude of the sinewave. If a trajectory does not excite state i then the sub-matrix associated with that trajectory is a 2×2 zero matrix.

Applying a least-squares solution [10] to (3.5) yields the following solution for the basis function coefficients.

$$\hat{\vec{\alpha}}_i \approx (\mathbf{B}_i^T\mathbf{B}_i)^{-1}\mathbf{B}_i^T(i\vec{1} - \mathbf{H}_i\vec{p}) \tag{3.6}$$

An expression for the estimated basis function coefficients for output code i , $\hat{\vec{\alpha}}_i$, in terms of the unknowns for all the trajectories, $\vec{p}$, has been determined. Keep in mind there are $2^n - 2$ of these equations but each equation has the same unknowns $\vec{p}$. Once an estimate of $\vec{p}$ is formed, the estimated basis coefficients of (3.6) can be calculated.

3.4.2.2 Constrained Least-Squares Solution

The final step in obtaining the estimated basis coefficients is to acquire an estimate of (GA) and $(G(c - x_o))$ or (p_1 and p_0) for all the trajectories. The problems associated with conventional methods [9] of obtaining $\vec{p}$ individually for each trajectory leads us to seek a different solution.

The new solution is as follows. Use the independent-based method [1] to estimate p_1 and p_0 for a single trajectory. The independent-based method finds a solution for the estimate of p_1 and p_0 that minimizes the sum-squared expected error of (2.1) and is shown as $\sum_{i=1}^{i=2^n-2} E_i^2$ or $\vec{E}^T\vec{E}$.

There are two expected error terms per output code i for a single trajectory as described by

$$\hat{E}_i^+ \;=\; i - h_i^{+jth}p_1^{jth} - p_0^{jth}$$

$$\hat{E}_i^- \;=\; i - h_i^{-jth} p_1^{jth} - p_0^{jth}.$$

$\hat{E}_i^+$ and $\hat{E}_i^-$ are the estimated expected errors based on positive and negative sloped sample sets. If the expected error terms are expanded over all output codes excited by the trajectory, the result is (3.7).

$$\hat{\vec{E}} = \vec{v} - \mathbf{H}_{fixed} \cdot \begin{bmatrix} p_0^{jth} \\ p_1^{jth} \end{bmatrix} \tag{3.7}$$

$$\mathbf{H}_{fixed} = \begin{bmatrix} 1 & h_1^{+jth} \\ 1 & h_1^{-jth} \\ 1 & h_2^{+jth} \\ 1 & h_2^{-jth} \\ \vdots & \vdots \\ 1 & h_{2^N-2}^{+jth} \\ 1 & h_{2^N-2}^{-jth} \end{bmatrix}, \quad \vec{v} = \begin{bmatrix} 1 \\ 1 \\ 2 \\ 2 \\ \vdots \\ 2^N - 2 \\ 2^N - 2 \end{bmatrix}$$

A least-squares solution minimizing $\vec{E}^T \vec{E}$ to estimate p_0^{jth} and p_1^{jth} yields the following solution [10].

$$\begin{bmatrix} \hat{p}_0^{jth} \\ \hat{p}_1^{jth} \end{bmatrix} = (\mathbf{H}_{fixed}^T \mathbf{H}_{fixed})^{-1} \mathbf{H}_{fixed}^T \vec{v} \tag{3.8}$$

An estimate of the unknown parameters for a single reference trajectory has now been determined and this estimate can be used as a constraint when solving for the remaining trajectory parameters.

Fig. 3.2 displays error versus slope for a single output code i. Each trajectory yields two points on the curve, one on the left and one on the right-hand

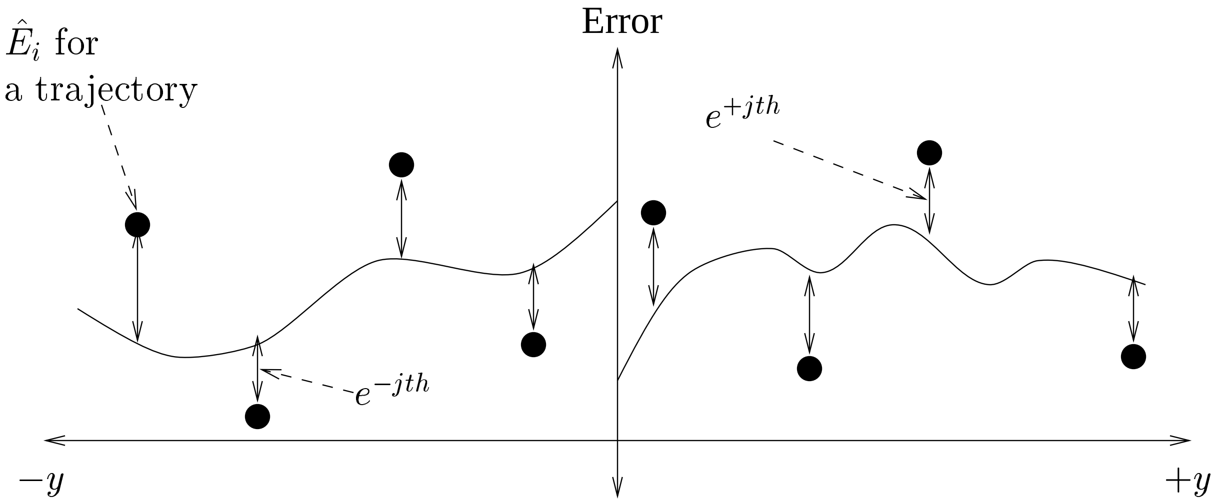

Figure 3.2: Theoretical error-vs-slope for output code i

side. This case shows a total of four trajectories. The estimated basis coefficients of (3.6) determine the shape of the curve in this figure. The distance from each point to the curve represents residual error from the error model for a given set of estimated basis coefficients. The points , except for the two points that correspond to the fixed reference trajectory, can be moved up or down vertically by varying $\vec{p}$. The estimate of $\vec{p}$ is selected to minimize the sum-squared residual error in our estimate of E_i (the distances between the points and curves of Fig. 3.2) over all output codes. Recall (3.6) which describes the basis coefficients as a function of $\vec{p}$. The error in this estimate of E_i is

$$\begin{aligned} \vec{\epsilon}_i &= (\mathbf{I} - \mathbf{P}_{\mathbf{B_i}})(i\vec{1} - \mathbf{H}_i\vec{p}) \\ \mathbf{P}_{\mathbf{B_i}} &= \mathbf{B}_i(\mathbf{B}_i^T\mathbf{B}_i)^{-1}\mathbf{B}_i^T \end{aligned} \tag{3.9}$$

The constrained least-squares estimate minimizes the sum-squared error of (3.9) under the constraint that p_0^{jth} and p_1^{jth}, of the reference trajectory, remain fixed.

The constrained least-squares setup is described by 3.10.

$$\mathcal{L}(\vec{p},\vec{\lambda}) = \sum_{i=1}^{2^N-2} \vec{\epsilon}_i^T \vec{\epsilon}_i + \vec{\lambda}^T \begin{bmatrix} \hat{p}_0^{jth} \\ \hat{p}_1^{jth} \end{bmatrix} \tag{3.10}$$

Substitution of (3.9) into (3.10) yields

$$\mathcal{L}(\vec{p},\vec{\lambda}) = \sum_{i=1}^{2^N-2} \left((\mathbf{I}-\mathbf{P}_{\mathbf{B_i}})(i\vec{1}-\mathbf{H}_i\vec{p})\right)^T \left((\mathbf{I}-\mathbf{P}_{\mathbf{B_i}})(i\vec{1}-\mathbf{H}_i\vec{p})\right) + \vec{\lambda}^T \begin{bmatrix} \hat{p}_0^{jth} \\ \hat{p}_1^{jth} \end{bmatrix}.$$

To obtain an estimate from (3.10), $\frac{d\mathcal{L}(\vec{p},\vec{\lambda})}{d\vec{p}} = 0$ and $\frac{d\mathcal{L}(\vec{p},\vec{\lambda})}{d\vec{\lambda}} = 0$ are evaluated. Setting $\frac{d\mathcal{L}(\vec{p},\vec{\lambda})}{d\vec{p}} = 0$ and solving for $\vec{p}$ gives

$$\hat{\vec{p}} = \left(\sum_{i=1}^{2^N-2} \mathbf{H}_i^T(\mathbf{I}-\mathbf{P}_{\mathbf{B_i}})\mathbf{H}_i\right)^{-1} \left(\sum_{i=1}^{2^N-2} \mathbf{H}_i^T(\mathbf{I}-\mathbf{P}_{\mathbf{B_i}})i\vec{1} - \frac{1}{2}\begin{bmatrix} 0 \\ 0 \\ \vdots \\ \lambda_1^{jth} \\ \lambda_2^{jth} \\ 0 \\ \vdots \end{bmatrix}\right). \tag{3.11}$$

Equation (3.11) describes $\hat{\vec{p}}$ in terms of $\vec{\lambda}$. Now solve for λ_1^{jth} and λ_2^{jth} that make p_0^{jth} and p_1^{jth} equal to the estimates obtained for the reference trajectory. Once λ_1^{jth} and λ_2^{jth} are found, $\hat{\vec{p}}$ can be calculated and substituted into (3.6) thus obtaining the estimated basis function coefficients, $\hat{\alpha}_{i,k}$.

3.5 Calibration Algorithm Summary

It is easy to get lost in the math involved with developing the error model of (2.7). This section outlines the procedure of collecting calibration data and estimating the basis function coefficients from those data.

1. Drive the ADC with several sinewaves at varying frequencies and amplitudes and collect sample sets for each input.
   (a) For each trajectory or sample set:
      i. Obtain an associated slope estimate of the samples and sort the samples into positive and negative slope sample sets.
      ii. Construct two histograms from each sample set and find h_i from (3.2) for each output code reached by the trajectory. Do this for both positive and negative sloped histograms.
      iii. Find the average slope associated with each output code i excited for both sample sets.
      iv. Evaluate $\vec{b}^T(y)$ of (3.3) for each average slope value y for both increasing and decreasing average slope sets.
2. At this point, the ADC has been driven by all the trajectories. The equations used to estimate the basis coefficients are setup as follows.
   (a) Create $\mathbf{H}_i$ and $\mathbf{B}_i$ of (3.5) for all output codes i.
   (b) Construct $\mathbf{P}_{\mathbf{B_i}}$ of (3.9) from $\mathbf{B}_i$ for all output codes i.
   (c) Estimate $\hat{p}_0^{jth}$ and $\hat{p}_0^{jth}$ for the fixed reference trajectory (jth trajectory).
      i. Construct $\mathbf{H}_{fixed}$ of (3.7) and estimate the fixed unknowns of (3.8).
   (d) Obtain an estimate of the unknowns for all trajectories, $\hat{\vec{p}}$, (given the jth trajectory is fixed) by evaluating $\frac{d\mathcal{L}(\vec{p},\vec{\lambda})}{d\vec{p}} = 0$ and $\frac{d\mathcal{L}(\vec{p},\vec{\lambda})}{d\vec{\lambda}} = 0$ and using (3.11).
   (e) Use $\hat{\vec{p}}$ to estimate the basis function coefficients of (3.6).

CHAPTER 4

Results

A method for obtaining a description of error as a function of input state and slope for a particular ADC has been developed. Once the error model has been determined, estimated error can be created for any given output code i and sample slope y. Estimated error can be used to compensate the output samples to accomplish dynamic error error correction for an ADC.

4.1 Compensating Samples

Compensating an output sample set of the ADC is straightforward. Obtain a sample set from the ADC and a slope estimate of the sample set. Take each element of the sample set along with its associated slope value and evaluate (2.7) to find the estimated expected error value. Subtract this error from the current element of the sample set. The result is a compensated sample set.

The following sections present results of this error compensation procedure. The results were compiled using both an 8-bit simulated folding ADC [8] and an 8-bit flash ADC using the Communication Laboratory's ADC test facility.

Both experimental and simulated results were obtained by calibrating the ADC with 50 trajectories, 10 frequencies and 5 amplitudes per frequency. The frequencies spanned evenly across the lower Nyquist band of the ADC being calibrated and the amplitudes were uniformly spaced from 50 to 95% of full scale loading. Estimated basis function coefficients used to obtain the following results were determined using the method described in Chapter 3.

4.2 ADC Simulation Results

Figures 4.1 to 4.3 show uncompensated and compensated magnitude spectra for a simulated 8-bit folding ADC [8]. The graphs illustrate the potential effectiveness of this error model and compensation technique. No other dynamic compensation techniques have provided the ability to remove high order harmonic distortion from such a complex model. The simulated ADC created error from complex functions of output code and slope only. Clearly, this method removes all distortion to the noise floor. Fig. 4.4 is a plot of a spurious free dynamic range (SFDR) for both compensated and uncompensated data for the simulated 8-bit folding ADC. The SFDR is a dynamic range test that measures the difference (in dB) between the fundamental and highest distortion component over the full Nyquist band for constant amplitude sine wave inputs. The results of Fig. 4.4 show excellent improvement over the entire Nyquist range. The highest distortion component over the range of this SFDR is at the noise floor. The error model developed in this thesis has clearly removed the error terms introduced by the simulated converter.

4.2.1 Removal of State and Slope Related Error

The error associated with uncompensated simulated results is strictly dependent upon output code and input signal slope. The error model developed in this thesis to estimate basis function coefficients is also strictly a function of output code and input signal slope. Simulated results suggest that the error model in this thesis can effectively remove state and slope dependent error from an uncompensated but repeatable ADC spectrum.

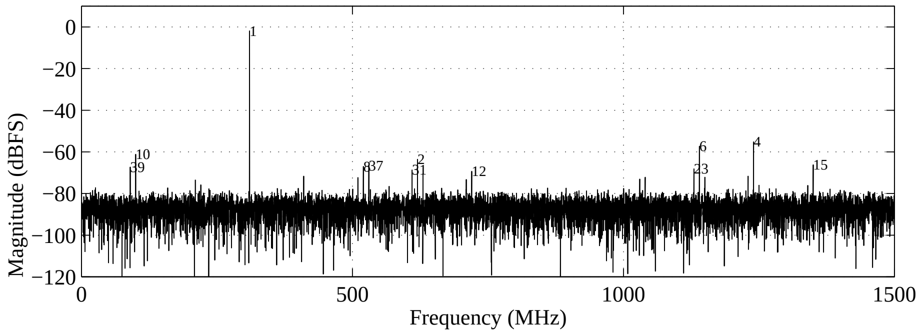

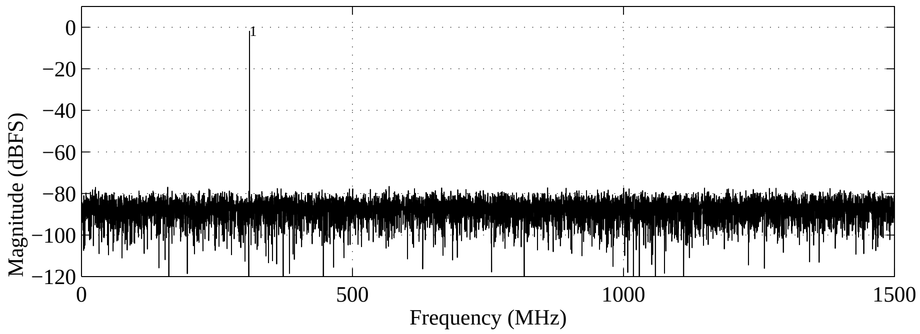

Figure 4.1: Uncompensated and compensated magnitude spectra, simulated results for a low frequency

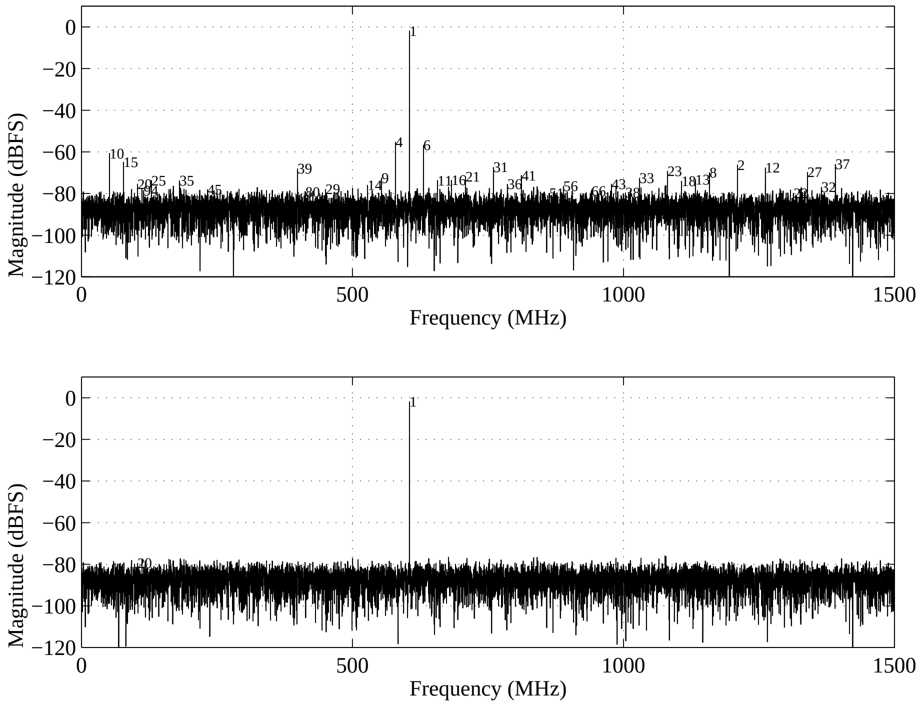

Figure 4.2: Uncompensated and compensated magnitude spectra, simulated results for a mid-Nyquist frequency

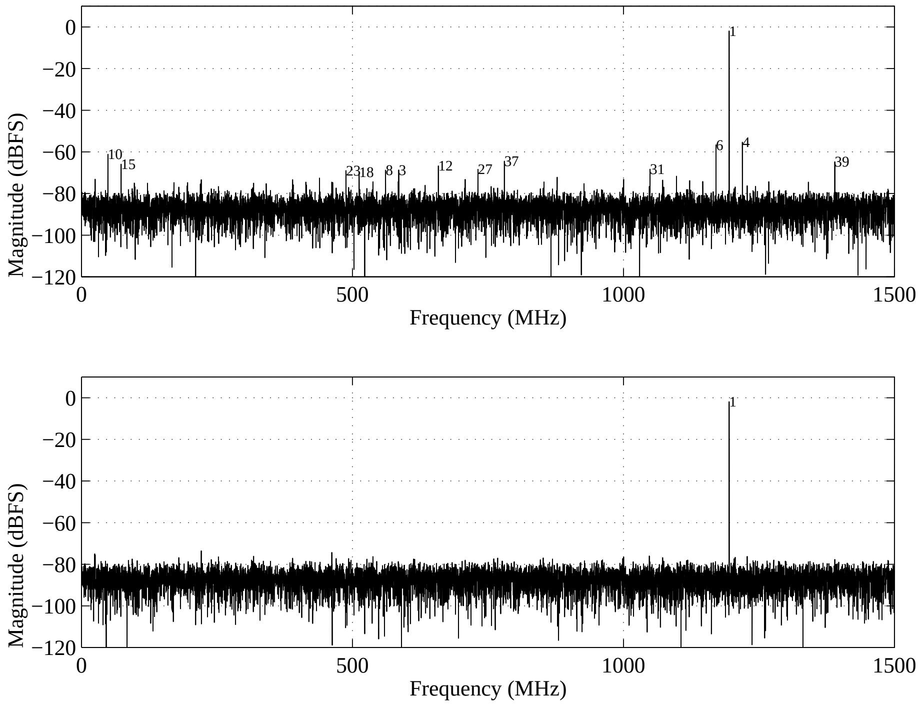

Figure 4.3: Uncompensated and compensated magnitude spectra, simulated results for a near-Nyquist frequency

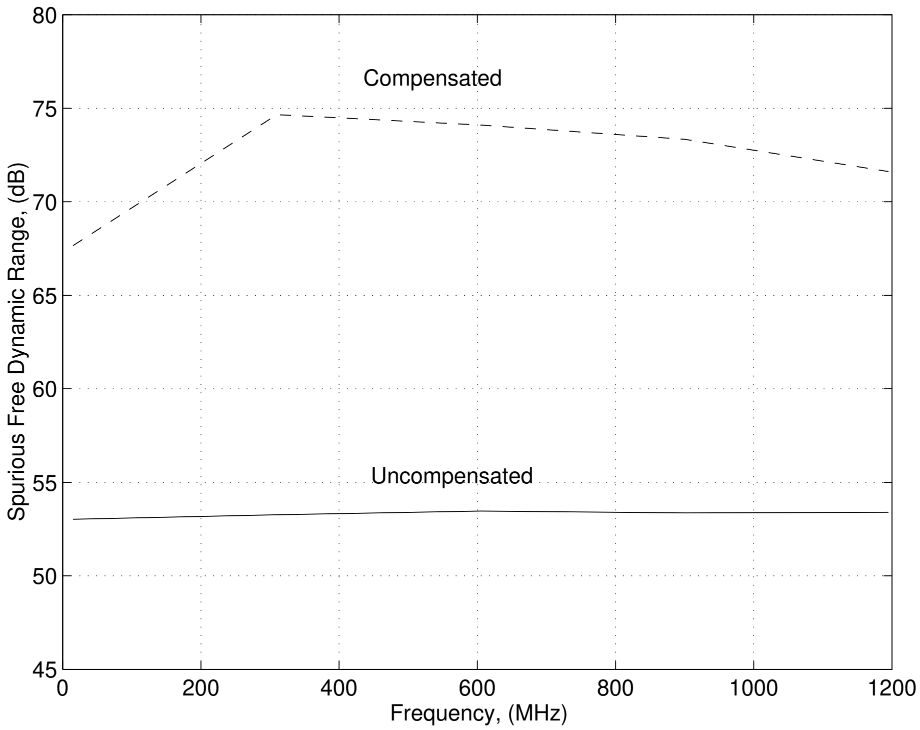

Figure 4.4: SFDR plot, simulated results

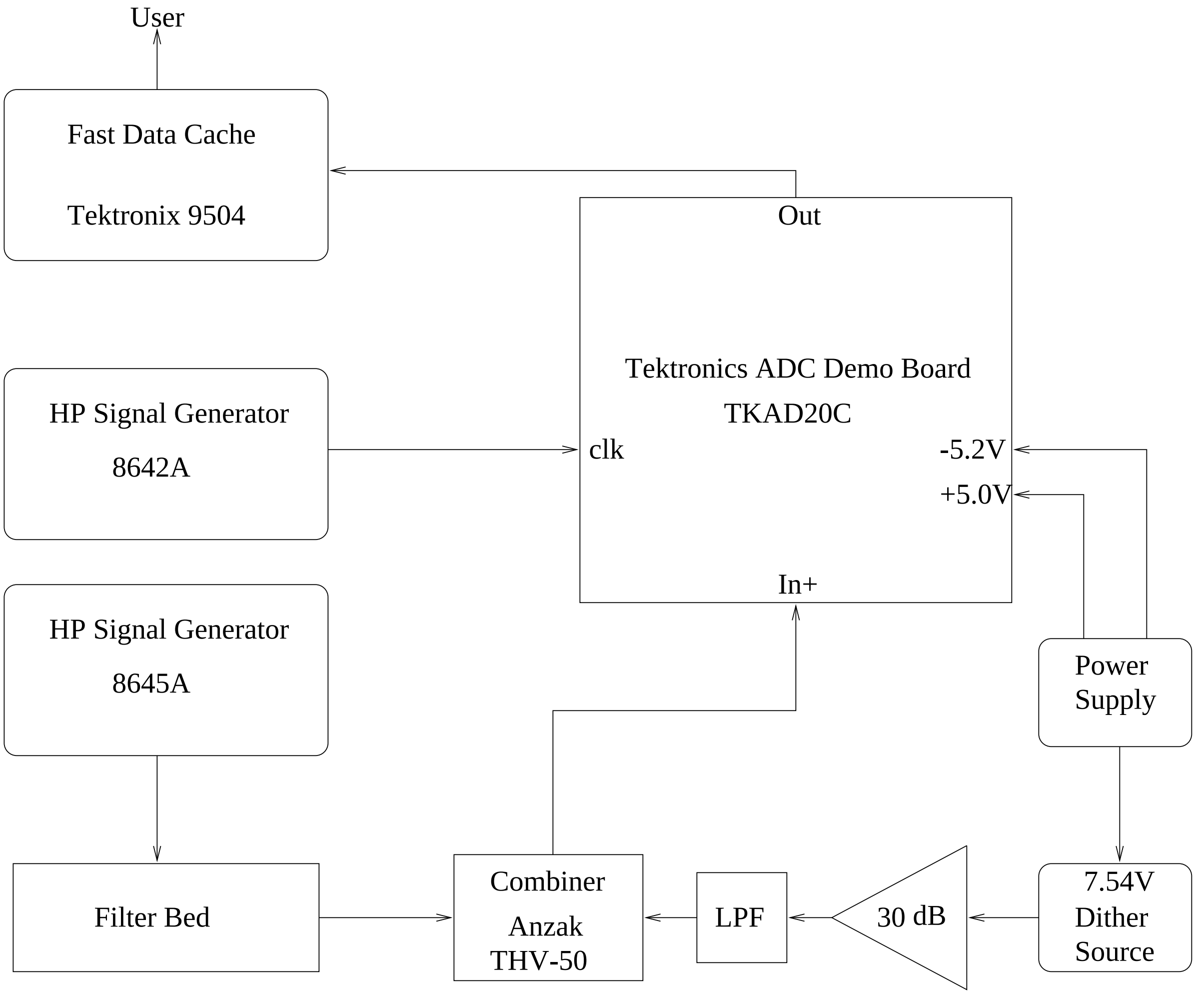

Figure 4.5: Communication laboratory's ADC test bed

4.3 Experimental ADC Results

Fig. 4.5 describes the setup used to extract uncompensated data from an ADC. The ADC evaluation board is an interface to the converter. Hewlett Packard signal generators are used to supply the ADC clock signal and to create sinusoidal inputs to the ADC. Each sinusoidal input is run through the filter bed to make sure that the ADC input signal is pure. Each filter contained within the filter bed is low pass. The filter is selected which allows the fundamental component to pass but all harmonic distortion components of the sinewave must lie in the stop-band of the filter. This insures that the input to the ADC is clean (harmonics below -100 dBFS) so that any distortion in the output samples has been introduced by the converter. The output of the filter bed is dithered before being applied to the input of the ADC. The purpose of adding dither to the input signal is to randomize quantization error. The dither signal is passed through a low pass filter with a cutoff frequency near Nyquist. The output of the ADC is stored in the Data Cache which can be retrieved by a workstation for data processing.

Figures 4.6 to 4.8 show uncompensated and compensated magnitude spectra for a real 8-bit flash ADC operated at 204.8 MSPS. The results are not as profound as the simulated results. Real ADCs contain errors that can not be accurately modeled as strictly a function of output code and signal slope but are functions of different parameters. Fig. 4.9 shows a spurious free dynamic range (SFDR) result for both compensated and uncompensated data for the ADC. The curve shows excellent improvement in performance across the full Nyquist band. To date (May 1997) this method has provided superior results compared to methods previously reported [6, 4].

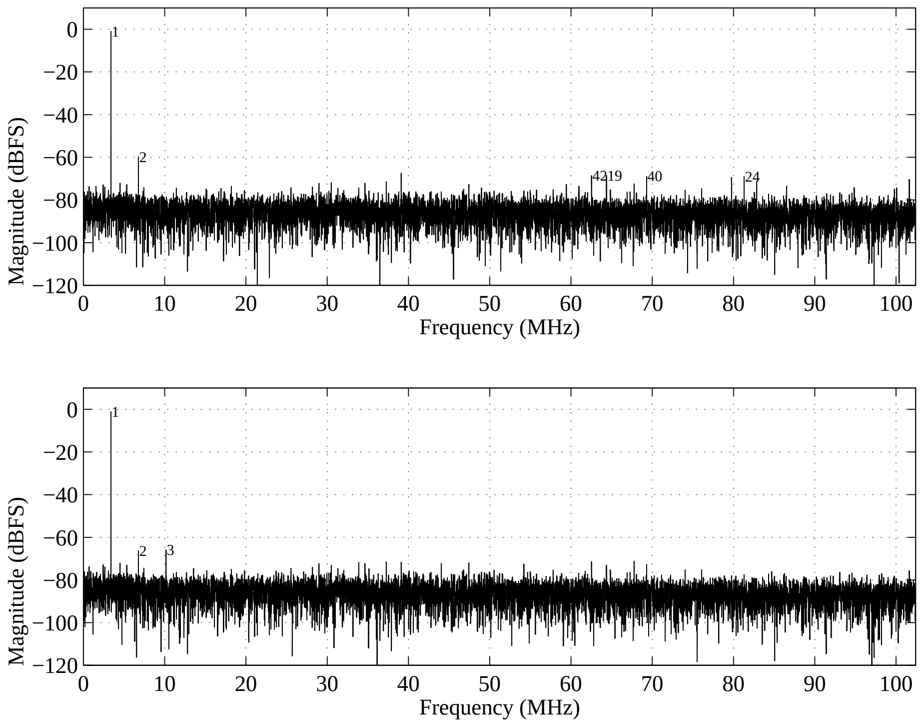

Figure 4.6: Uncompensated and compensated magnitude spectra, experimental results for a low frequency

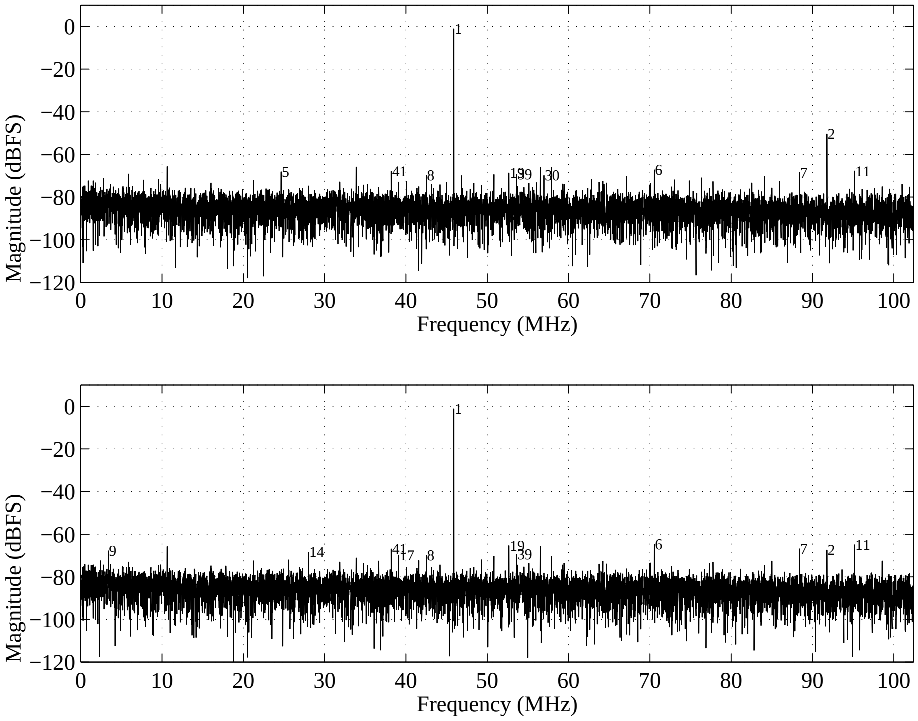

Figure 4.7: Uncompensated and compensated magnitude spectra, experimental results for a mid-Nyquist frequency

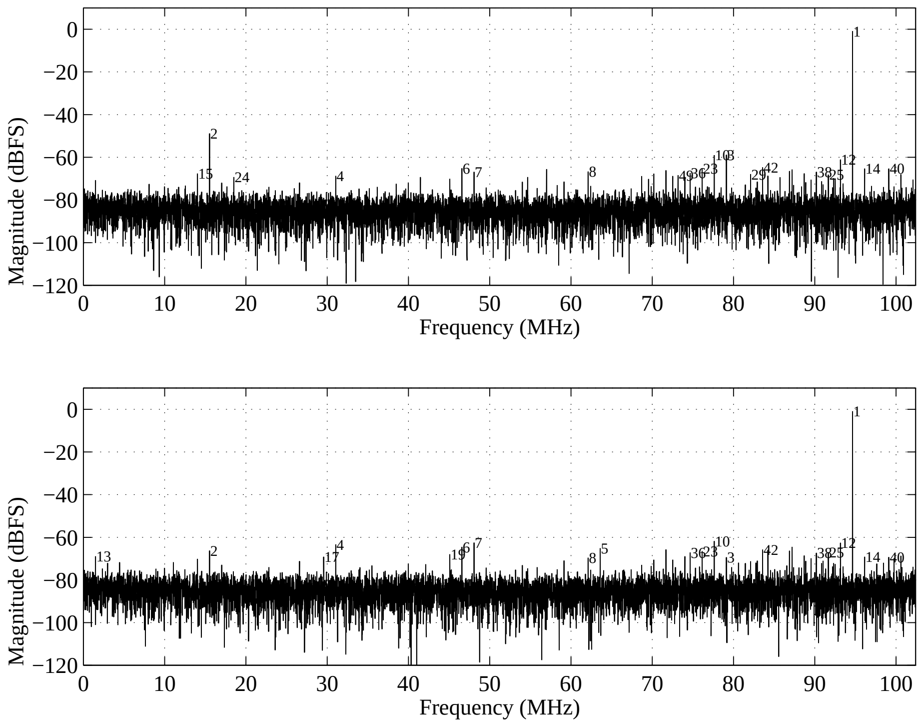

Figure 4.8: Uncompensated and compensated magnitude spectra, experimental results for a near-Nyquist frequency

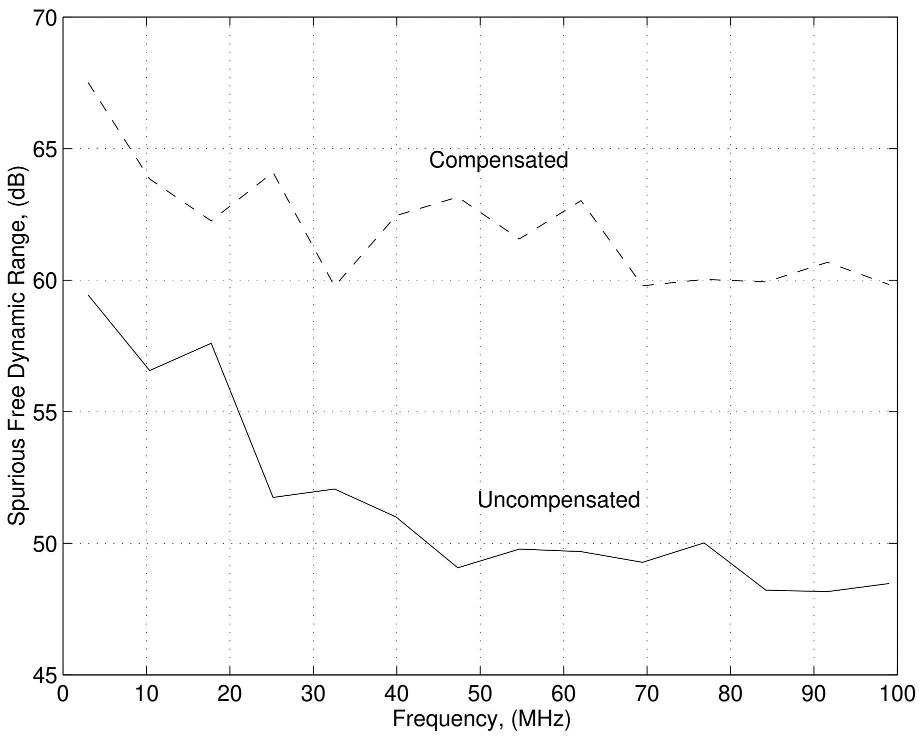

Figure 4.9: SFDR plot, experimental results

CHAPTER 5

Conclusions

This thesis developed a new error model to represent output code and slope dependent ADC errors. A calibration method to obtain data that accurately describe an ADC according to the dynamic error model was also developed. The validity of the error model was evaluated by means of error compensation on a simulated ADC whose error contained complex functions of state and slope only. Experimental results were obtained from an 8-bit flash ADC using the communication laboratory's test bed.

The dynamic error model consists of an error function of slope for each ADC output code. The high resolution of the error model accurately represents discontinuous expected error vs output code patterns as required by the experiment shown in Chapter 2. Estimates of quantization thresholds were obtained using the sinewave histogram method and the histogram information was used in solving for the basis function coefficients at each output code.

Once a dynamic error model was defined, a calibration method was developed to extract data from the ADC when excited over its full range of output codes and slopes. An array of sinusoidal signals with varying frequencies and amplitudes was passed through the ADC and output sample sets were processed. The amplitudes and frequencies were selected to fill the slope vs output code space of the ADC. The transformation of calibration data to an estimate of basis function coefficients was developed. By setting the dynamic error model for state i equal to the expected error of that state, a least-squares solution for the basis function coefficients as a function of the unknowns (GA) and $(G(c - x_o))$ was determined.

The simulated 8-bit ADC contained complex state and slope dependent error only. Results showed that this compensation method is highly effective for removing all errors that depend on state and slope. The results demonstrated by this method for real ADCs are not as profound. However, broadband improvements have been obtained which match or exceed all previous results for this converter. The exact mechanisms that create ADC error are not always known and often rely on more than just current state and slope. By studying residual errors which remain after this compensation, it will be possible to discover other variable dependencies for the remaining errors.

References

[1] IEEE Standard 1057, standards for digitizing waveform recorders. Technical report, National Institute of Standards and Technology, July 1989.

[2] W. Ahmed. Fast orthogonal search for training radial basis function neural networks. Master's thesis, University of Maine, Dept. of Electrical and Computer Eng., Orono Maine, August 1994.

[3] R.M. Gray and T.G. Stockham, Jr. Dithered quantizers. *IEEE Trans. Inform. Theory*, IT-39:805–812, May 1993.

[4] D.M. Hummels, F.H. Irons, R. Cook, and I Papantonopoulos. Characterizaion of ADCs using a non-iterative procedure. In *Proceedings of IEEE International Symp. on Circuits and Systems*, London, May 1994.

[5] D.M Hummels, I.N. Papanonopoulos, and F.H. Irons. Identification of error mechanisms in a folding and interpolating ADC. In *Proceedings of IEEE International Symp. on Circuits and Systems*, Atlanta, May 1996.

[6] F.H. Irons, D.M. Hummels, and S.P. Kennedy. Improved error compensation for analog-to-digital converters. *IEEE Trans. Circuits and Systems*, 38:958–961, June 1991.

[7] F.H. Irons, D.M. Hummels, and I.N. Papantonopoulos. ADC error diagnosis. In *Proceedings of IEEE International Instumentation and Measurement Technology Conference*, Brussels, June 1996.

[8] F.H. Irons, D.M Hummels, and C.A. Zoldi. ADC architectural diagnostic testing procedures. In *Proceedings of Government MicroCircuit Applications Conference*, Orlando, March 1996.

[9] I.N. Papantonopoulos. Error modeling for folding and interpolating analog to digital converters. Master's thesis, University of Maine, Dept. of Electrical and Computer Eng., Orono Maine, August 1995.

[10] L.L. Scharf. *Statistical Signal Processing: Detection, Estimation, and Time Series Analysis.* Addison-Wesley, Reading, Massachusetts, 1991.

Biography of the Author

Jonathan Larrabee was born in Portland, Maine on March 17, 1973. He received his high school education from Greely High School in Cumberland in 1991.

He entered the University of Maine in 1991 and obtained his Bachelor of Science degree in Electrical Engineering in 1995.

In May 1995, he was enrolled for graduate study in Electrical Engineering at the University of Maine and served as Research Assistant and was employed as a Resident Assistant at Oxford Hall durring both years of graduate school. His current research interests include communications and signal processing. His interests include mountain biking, alpine skiing, and music. He is a candidate for the Master of Science degree in Electrical Engineering from the University of Maine in August 1997.